Hollow zeolite microspheres as a nest for enzymes: a new route to multifunctional heterogeneous catalysts

Valentin Smeets,[a] Walid Baaziz,[b] Ovidiu Ersen,[b] Eric M. Gaigneaux,[a] Cédric Boissière,[c] Clément Sanchez,[c] and Damien P. Debecker*[a]

[a] Institute of Condensed Matter and Nanosciences (IMCN), UCLouvain Place L. Pasteur 1, 1348 Louvain-la-Neuve, Belgium E-mail: damien.debecker@uclouvain.be

[b] Institut de Physique et Chimie des Matériaux de Strasbourg (IPCMS), UMR 7504 CNRS – Université de Strasbourg 23 rue du Loess, 67034 Strasbourg Cedex 2, France

[c] Laboratoire Chimie de la Matière Condensée de Paris (LCMCP), Sorbonne Université, CNRS, Collège de France, PSL Research University 4 Place Jussieu, F-75005 Paris, France

Electronic Supplementary Information

1. Experimental Procedures

1.1. Preparation and characterization of the inorganic catalyst

The hollow zeolite microspheres were obtained via a two-step preparation route (see Scheme 2a). First, a stable **TS-1** colloids suspension (*ca.* 10 wt. %) was prepared by hydrothermal synthesis according to a procedure adapted from the literature.[1] 0.55 g of titanium isopropoxide (TiiP, Acros Organics, ≥ 98%), was first solubilized in 5 g of ^{i}PrOH (VWR) (Solution A). In a separate vessel, 22.5 g of tetraethylorthosilicate (TEOS, Sigma-Aldrich, 98%) was mixed with 16.41 g of 40 wt. % aqueous tetrapropylammonium hydroxide (TPAOH, Merck) and 9.84 g of distilled H_2O (Solution B). Both solutions were stirred for 5 min at room temperature. Solution A was then added dropwise to Solution B, and the turbid mixture was stirred for 15 min until a clear yellowish solution was obtained. After that, 5.47 g of TPAOH (40 wt. % aq.) diluted in 38.28 g of distilled H_2O was added. The initial gel composition was 1 SiO_2: 0.018 TiO_2: 0.40 TPAOH: 32 H_2O with a Ti loading of 1.8% (here and after, the Ti loading is expressed as "mol Ti / (mol Ti + mol Si) × 100 %"). The solution was then kept under stirring at 75°C for 3h – in order to reduce the volume of the solution by evaporation of the alcohol. Then, 30 g of distilled H_2O was added and the resulting mixture was transferred into a 70 ml Teflon-lined stainless steel autoclave for 24 h at 160°C. After rapid cooling, the obtained white precipitate was isolated by centrifugation, thoroughly washed with distilled H_2O until neutral pH, and finally suspended in 37.5 g of distilled H_2O while kept under stirring at room temperature.

In a second stage, this suspension was mixed with 10.29 g of a clear silica precursor solution prepared as follows: 4.90 g of distilled H_2O was first added to 1.19 g of TPAOH (40 wt. % aq.) under stirring, followed by the subsequent addition of 3.26 g of TEOS. The resulting solution was kept overnight under vigorous stirring to hydrolyze the precursors, and was further aged for 6 h at 80°C in a closed vessel. 0.94 g of Pluronic® F127 (Sigma-Aldrich) was then added and the solution was thoroughly mixed for 1 h. The composition of the resulting clear yellowish solution was 1 SiO_2: 0.15 TPAOH: 0.005 F127: 20 H_2O.

The mixture was stirred for 30 min and subsequently sprayed by a Büchi Mini Spray Dryer B-290 with an air pressure of 4 bars. The aerosol was dried by passing through a glass reactor heated at 80°C. The obtained powder was treated at 70°C overnight and then calcined at 550°C for 5 h (5°C/min). We obtained 4.57 g of the final material, which was denoted "**TS-1_Aer**".

As a reference material, **TS-1** nanocrystals were isolated after centrifugation of the 10 wt. % suspension mentioned above, followed by drying in air at room temperature for 72 h and calcination at 550°C for 5 h (5°C/min). This reference catalyst was denoted "**TS-1**".

The Ti content of the materials was measured by ICP-AES on an ICP 6500 instrument (Thermo Scientific Instrument) after dissolution of the samples by sodium peroxide fusion. XPS experiments were carried out using an SSX 100/206 spectrometer (Surface Science Instruments, USA) with Al-Kα radiation operated at 10 kV and 20 mA. The binding energy scale was calibrated on the Si 2p peak, fixed at 103.5 eV.[2] The quantification of Ti in Ti–O–Si and Ti–O–Ti was based on the decomposition of the $2p_{3/2}$ peak at 460.0 and 458.5 eV, respectively.[3,4] Si was quantified on the basis of the Si 2p peak. Powder X-ray diffraction (PXRD) patterns were recorded at room temperature on a Siemens D5000 diffractometer equipped with a Ni filter using CuKα radiation (Bragg-Brentano geometry) operated at 40 kV and 40 mA. Diffractograms were taken between 5° and 80° (2θ) with a step size of 0.02° (2θ). DRUV-vis spectra were recorded on a Varian Cary 5000 UV–Vis–NIR Spectrophotometer equipped with a Harrick single-beam Praying Mantis Diffuse Reflectance collection system. The spectra were recorded at room temperature in the 12500–50000 cm^{-1} range. Spectralon® Diffuse Reflectance Standard was used to measure the background spectrum. The DRUV-vis spectra were background corrected and the Kubelka-Munk function *F(R)* was used to display the data. Scanning electron microscopy (SEM) images were taken using a JEOL 7600F microscope at 15 kV voltage. Samples were pre-treated with a chromium sputter coating of 15 nm carried out under vacuum with a Sputter Metal 208 HR (Cressington). Particle size distribution was estimated from a SEM image recorded at 2500 × magnification (N = 293). SEM-FEG pictures were obtained with a Hitachi SU-70. Scanning transmission electron microscopy (STEM) analysis was carried out using a JEOL 2100 FEG S/TEM microscope operated at 200 kV and equipped with a probe spherical aberration corrector. The sample was dispersed in ethanol and deposited on a holey carbon coated TEM grid. For the STEM-ADF (annular dark field) analysis, a spot size of 0.13 nm, a current density of 140 pA, a camera focal length of 8 cm, corresponding to inner and outer diameters of the annular detector of about 73 and 194 mrad, were used. For the Electron tomography (ET), the TEM grid containing the sample was introduced and fixed inside a specific sample holder. The acquisition of tilt series was acquired using the tomography plug-in of the Digital Micrograph software, which controls the specimen tilt step by step, the defocusing and the specimen drift. The ADF and BF tilt series in the STEM were acquired by using the ADF and BF detectors and tilting the specimen in the angular range of ± 66° using an increment of 2° in the equal mode, giving thus a total number of images equal to 65 images in each series. The inner radius of the ADF detector was about 40 mrad, a relatively large value that allows us to consider that the intensity in the corresponding images is proportional to the mean atomic number of the specimen in a first approximation. The recorded images were spatially aligned by cross correlating consecutive images using IMOD software. The volume calculation was realized using the algebraic reconstruction technique (ART) implemented in the TomoJ plugin working in the ImageJ software. Finally, the visualization and the analysis of the obtained volumes were carried out using the displaying capabilities and the isosurface rendering method in the Slicer software. Textural properties were determined from

N_2 adsorption/desorption isotherms at -196°C using a Tristar 3000 instrument (Micromeritics, USA). Prior to measurement, the calcined samples were first degassed overnight under vacuum at 150°C. For the hybrid catalyst **GOx_25@TS-1_Aer**, the centrifuged catalyst suspension was dried overnight at 120°C under vacuum prior to degassing. The external specific surface area – which includes the specific surface area of mesopores – was evaluated by the slope of the line drawn in the linear portion of the t-plot in the 3.5–5 Å thickness range; the micropore volume was given by the intercept. The total pore volume was measured at P/P_0 = 0.98. The pore size distribution (PSD) was obtained from the adsorption branch of the isotherm using the BJH method. Mercury porosimetry measurements were carried out on a Micromeritics Autopore IV apparatus.

The catalytic performance of the inorganic catalysts was tested for the conversion of allyl alcohol into glycidol in H_2O with hydrogen peroxide as the oxidizing agent. The reaction was carried out in a two-necked glass round-bottomed reactor at 45°C, equipped with a condenser, a magnetic stirrer and a rubber septum. In a typical run, 0.528 g (0.9 M) of allyl alcohol (Acros Organics, 99%), 0.037 g (0.05 M) of butan-1-ol (Sigma-Aldrich, ≥ 99.4%) – used as the internal standard – and 50 mg (5 $g.l^{-1}$) of catalyst were pre-mixed in 9.152 g of distilled H_2O under stirring. After 10 min, 0.204 g (0.18 M) of 30 wt. % aqueous H_2O_2 was added and the mixture was allowed to react for 3 h. The product formation was followed by collecting aliquots at regular time intervals and by analyzing them in gas chromatography, using a Varian CP-3800 chromatograph equipped with a FID detector and a capillary column (BR-5, 30 m, 0.32 mm i.d., 1.0 µm film thickness). Prior to injection, water was removed by extraction with ethyl acetate (50:50 v/v).

Catalyst recyclability has been assessed on three consecutive measurements on **TS-1** and **TS-1_Aer**. After each catalytic test, the catalysts were recovered by filtration, dried overnight at 120°C under vacuum and calcined at 550°C for 5h (5°C/min). The hot filtration test was carried out by removing the catalyst after 45 min reaction time; the filtrated reaction mixture was then allowed to react for an additional 2 h 15 min.

1.2. Characterization of the enzyme

Glucose oxidase (**GOx**) from *Aspergillus niger*, in powder form, was purchased from TCI. The activity of the enzyme was determined on the basis of the oxygen consumption, which was monitored using an OXY-4 mini fiber optic oxygen meter connected to an optical oxygen sensor (PreSens GmbH, Germany) glued on the inner side of a closed reaction vessel equipped with a magnetic stirrer.[5] The procedure for the determination of the activity is as follows: first, the reaction medium – composed of 200 mM D-glucose dissolved in 10 mM pH buffer – was saturated with O_2 by sparging the medium with air or oxygen (Air Liquide Alphagaz 1, purity 5.0). The glucose concentration was chosen so that it was not limiting for the enzymatic activity (the Michaelis-Menten constant for D-glucose is only 26 mM[6]). The assay was then initiated by the addition of **GOx**. The specific enzymatic activity, approximated by the initial O_2 consumption rate (see one example in Figure S1), is expressed relatively to the amount of enzyme, *i.e.* µmol $O_2.min^{-1}.mg^{-1}$ or $U.mg^{-1}$, where U is the symbol for the activity unit. The amount of enzyme was chosen so that it allows for an accurate determination of the enzymatic activity,[7] in accordance with the response time of the instrument. The enzyme was tested in various conditions of pH and temperature (Figure S2).

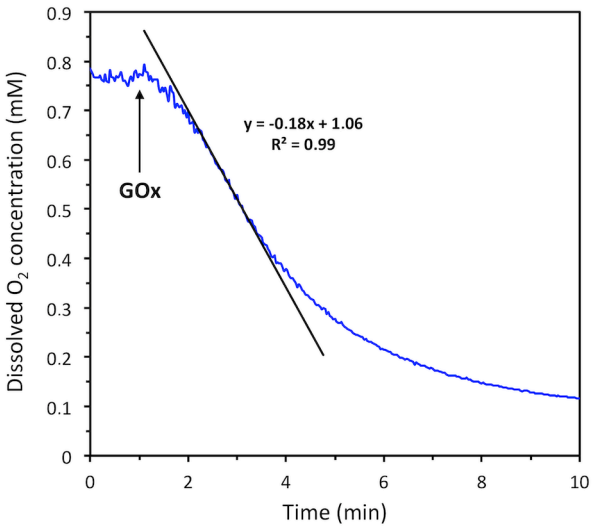

Figure S1. Illustration of the method used to evaluate the specific enzymatic activity of **GOx** using kinetic data for the consumption of oxygen. Experimental conditions: T = 45°C, 10 mM phosphate buffer pH 7.0, [D-glucose] = 200 mM, 0.15 mg free **GOx**, 100 ml reaction medium. The enzymatic activity is approximated by the initial oxygen consumption rate. The enzyme is introduced at *ca.* 1 min, as illustrated by the position of the arrow.

Example of calculation of the specific enzymatic activity (*E*) for free **GOx** at 45°C (see Figure S1):

$$E = \frac{\text{initial mol of } O_2 \text{ converted per minute}}{\text{mass of } \mathbf{GOx}} = \frac{0.18\ \left[\text{mmol } O_2.l^{-1}.min^{-1}\right]\ 0.1\ [l]\ 10^3\ [\mu\text{mol } O_2.\text{mmol } O_2^{-1}]}{0.15\ [\text{mg}]} = 120\ \mu\text{mol } O_2.min^{-1}.mg^{-1} = 120\ U.mg^{-1}$$

Where 0.18 mmol $O_2.l^{-1}.min^{-1}$ is the slope of the tangent to the curve in Figure S1.

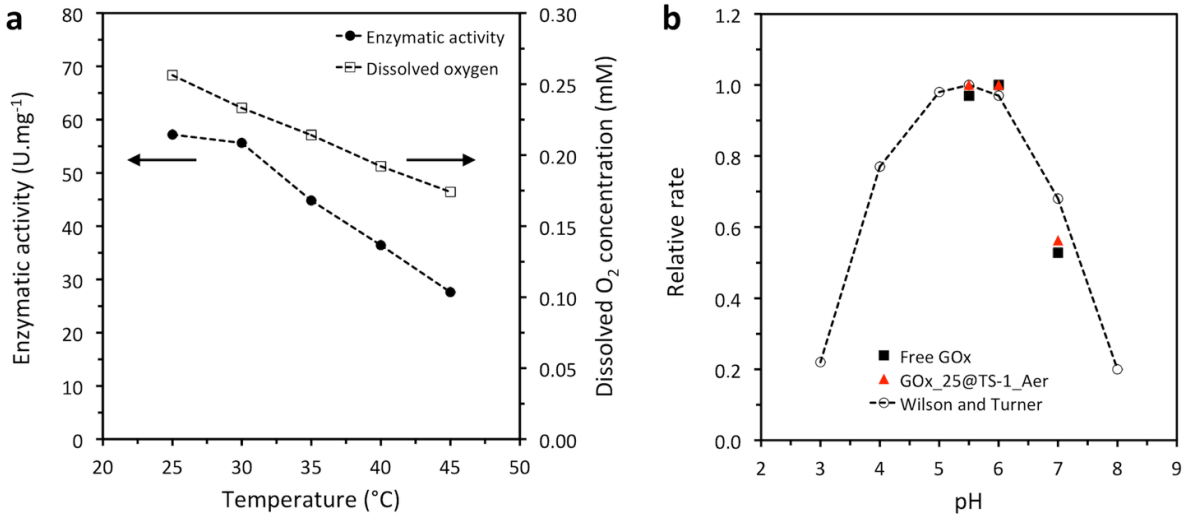

Figure S2. (a) Temperature dependence of free **GOx** activity and dissolved oxygen concentration. Experimental conditions: 10 mM phosphate buffer pH 7.0, [D-glucose] = 200 mM, reaction medium fed with air. A particular attention has been paid to the operational conditions required to maintain a high enzymatic activity. Generally speaking, epoxidation reactions are carried out at moderate temperatures (*e.g.* 45–90°C), whereas enzymes usually work under milder conditions (*e.g.* 25–45°C). In air, the enzyme was shown to be active in 25–45°C temperature range. However, the activity decreased almost linearly with the temperature. Since the dissolved oxygen concentration decreases as the temperature increases, we surmise that the decrease of the enzymatic activity is partially due to the depletion of oxygen – accordingly with Michaelis-Menten model and the reported value for k_{mO} (see below) (0.2 mM).[8,9] This is further supported by the results shown in Figure 4c which indicate that the activity is about two fold higher at 25°C (143 *vs.* 57 $U.mg^{-1}$) by replacing air with oxygen and thus by increasing the dissolved oxygen concentration (1.21 mM vs. 0.26 mM). At such high dissolved oxygen concentration, we can surmise that the enzyme is close to its maximum reaction rate. Therefore, increasing the temperature to 45°C has a lower impact on the activity in that case (116 $U.mg^{-1}$, 0.77 mM O_2), with benefit for the combination of **GOx** with the inorganic catalyst, (b) relative enzymatic activity of free **GOx** and **GOx** in **GOx_25@TS-1_Aer** measured at various pH. Experimental conditions: T = 45°C, 10 mM citric acid-phosphate (pH 5.5–6.0) or phosphate (pH 7.0) buffer, [D-glucose] = 200 mM. Empty markers refer to data from Wilson and Turner.[10] It appears that the activity is higher at pH 5.5–6.0 compared to pH 7.0. This is consistent with literature data that report a maximal activity at pH 5.5. From the literature data, one can also notice that the activity rapidly decreases when pH is lower than 5.0, which implies that pH control is important for practical applications.

Soluble enzyme concentration was evaluated by a modified Bradford titration method.[11,12] Calibration was done by mixing 0.5 ml of standard solutions of **GOx** within 0–0.1 $mg.mL^{-1}$ concentration range with 0.5 ml of Bradford reagent (Sigma-Aldrich). The absorbance was measured at 590 and 450 nm using a Thermo Scientific Genesys 10s Vis spectrophotometer and values of A_{590}/A_{450} were plotted against **GOx** concentration.

1.3. Enzyme immobilization

The enzyme was entrapped in **TS-1_Aer** *via* precipitation and cross-linking (Scheme 2b, see also pictures in Figure S3) following a two-step procedure: 1) 500 mg of **TS-1_Aer** was impregnated with 3 ml of freshly prepared **GOx** solution with concentration in the 2.5–25 $mg.mL^{-1}$ range. The suspension was gently stirred using a rotating agitator set at 50 rpm for 15 min. Vacuum was then applied in order to remove air bubbles trapped in the pores of the material and to force the enzyme solution into the voids of the particles. The excess liquid was subsequently removed by centrifugation at 10,000 g for 10 min. 2) 9 ml of ethyl lactate was added to the pellet as a precipitation agent (final volume fraction of 0.9) and the suspension was stirred at 50 rpm using the rotating agitator. After 30 min, 390 µl of glutaraldehyde (GAH, final concentration of 100 mM) was added to the suspension which was further stirred for 2.5 h.[13] The suspension was then allowed to rest overnight at 4°C. Then, the wet powder was centrifuged and washed with distilled H_2O until no enzyme was present in the supernatant (activity and Bradford assays). The final materials were denoted "**GOx_X@TS-1_Aer**", where *X* = 2.5–25 stands for the concentration of the enzymatic solution used during the impregnation step. The wet solids were suspended in 10 ml of distilled H_2O and stored at 4°C prior to use. Additionally, two blank materials were prepared i) using the same immobilization protocol without **GOx** ("**GOx_0@TS-1_Aer**"), ii) replacing ethyl lactate and GAH by distilled H_2O when using 25 $mg.mL^{-1}$ **GOx** solution ("**GOx_25@TS-1_Aer_b**").

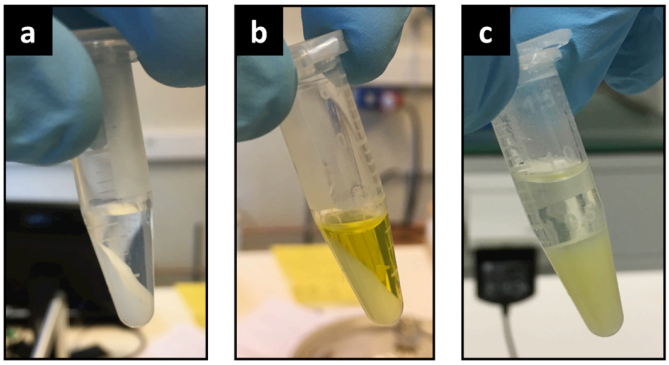

Figure S3. Pictures illustrating the enzyme immobilization procedure (Scheme 2b). In (a), the **TS-1_Aer** catalyst is suspended in distilled water without enzymes (blank). In (b), the solid is suspended in a solution of **GOx** (impregnation step). In (c), the impregnated solid shown in (b) is recovered by centrifugation and suspended in a ethyl lactate/glutaraldehyde mixture (precipitation and cross-linking steps). The yellowish colour of the pellet indicates the presence of enzymes in the solid (the refractive index of ethyl lactate is close to that of silica) whereas the supernatant is almost colorless.

The enzyme loading in **GOx_X@TS-1_Aer** was evaluated by thermogravimetric analysis (Figure S4) using a TGA/DSC 3^+ (Mettler Toledo) thermogravimetric apparatus operating under air at a heating rate of 10°C.min^{-1}. Prior to measurement, the solid materials – obtained by centrifugation of the suspensions – were dried overnight at 120°C under vacuum. **GOx** powder as well as **GOx_0@TS-1_Aer** ("Blank" in Figure S4) were used as reference materials. Alternatively, the loading of **GOx** in **GOx_25@TS-1_Aer_b** was determined by deducting the amount of soluble enzyme in the washing fractions (Bradford assay).

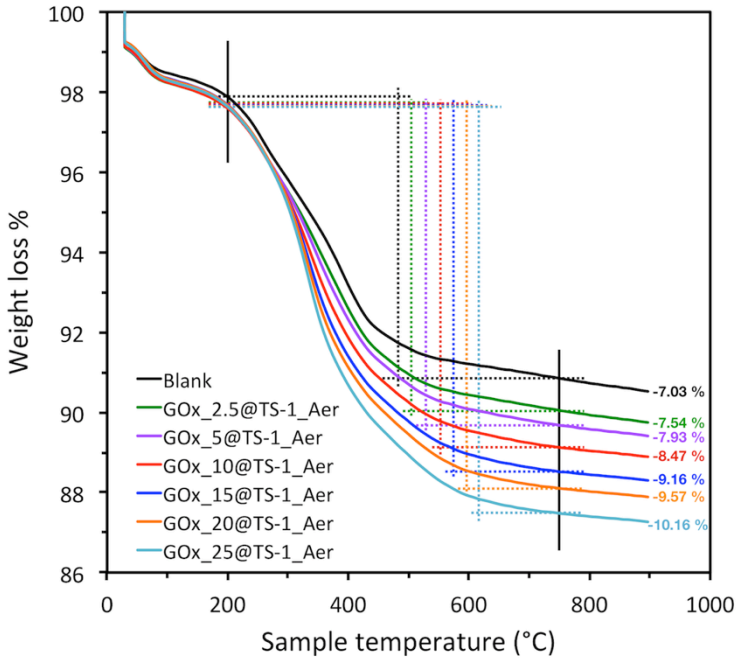

Figure S4. Determination of the experimental enzyme loading by TGA analysis. **GOx_0@TS-1_Aer** (Blank) was used as reference material. The temperature interval 200–750°C was selected on the basis of the TGA curve obtained with commercial **GOx** powder (*not shown*).

Example of calculation of the experimental enzyme loading in **GOx_25@TS-1_Aer**:

$$\text{Exp. loading} = \frac{10\,(\text{Weight loss \% Sample - Weight loss \% Blank})[\text{mg}_{\text{GOx}}.\text{g}^{-1}]}{\text{Weight loss \% GOx / 100}} = \frac{10\,(10.16\text{-}7.03)\,[\text{mg}_{\text{GOx}}.\text{g}^{-1}]}{84.5\,/\,100} = 37\ \text{mg}_{\text{GOx}}.\text{g}^{-1}$$

Where "Weight loss % GOx" is the weight loss of **GOx** in the temperature interval 200–750°C. It corresponds to a value of 84.5%.

The amount of glutaraldehyde bound to the enzyme is neglected in the above calculations, as it is reported to be limited to a few percents of the enzyme mass.[14]

Example of calculation of the nominal enzyme loading in **GOx_25@TS-1_Aer**:

$$\text{Nom. loading} = \frac{[\text{GOx}]\left[\text{mg}_{\text{GOx}}.\text{ml}^{-1}\right] V_{imp}\ [\text{ml}]\text{CF}}{\text{Mass of solid [g]}} = \frac{25\left[\text{mg}_{\text{GOx}}.\text{ml}^{-1}\right] 0.7\ [\text{ml}]1.43}{0.5\ [\text{g}]} = 50\ \text{mg}_{\text{GOx}}.\text{g}^{-1}$$

Where "[GOx]" is the enzyme concentration in the impregnation solution (= *X*), "CF" is a concentration factor that takes into account the partial evaporation of the impregnation solution under vacuum, "V_{imp}" is the volume of impregnation solution remaining in the 500 mg of **TS-1_Aer** after elimination of the excess of liquid by centrifugation.

The enzyme heterogeneization was addressed by a filtration test carried out by removing the solid particles by centrifugation and filtration (0.2 µm syringe filter) and then measuring the enzymatic activity in the filtrate.

1.4. Chemo-enzymatic epoxidation of allyl alcohol

The cascade reaction (Scheme 1) was run at 45°C in a 100 ml homemade glass reactor equipped with a thermostatic bath and a magnetic stirrer (Figure S5). The reaction medium was composed of 5.28 g of allyl alcohol (0.9 M), 0.373 g of butan-1-ol (50 mM, internal standard) and 81.46 ml of 200 mM D-glucose solution. This reaction medium was fed with oxygen using a PDMS hollow fiber module (PDMSXA-2500, MedArray, USA) connected to the reactor by a low shear stress pump operating at a liquid flow rate of 100 ml.min^{-1} (lumen side) and fed with oxygen at 1 l.h^{-1} sweep rate (shell side). After reaching temperature equilibrium, 11.9 ml of a suspension containing **GOx** and the inorganic catalyst (final concentration of 5 g.l^{-1}) – either in the form of the **GOx_25@TS-1_Aer** and **GOx_2.5@TS-1_Aer** hybrid catalysts or a mechanical mixture of **TS-1_Aer** and free **GOx** – was added and the 100 ml mixture was allowed to react for 24 h. During reaction, acidification by gluconic acid product was compensated by automatic titration with 0.5 M NaOH using a TitroLine 7000 automatic titrator (Xylem Inc., Germany) equipped with the "pH-stat" mode. The pH value was maintained in the 5.5–6.0 range. Glycidol formation was followed by gas chromatography, whereas the glucose conversion was evaluated by the amount of base added. H_2O_2 concentration was measured *via* a colorimetric assay with 15% w/v titanium(IV) sulfate (Fisher Chemical) on aliquots taken at regular intervals.[15] Absorbance was measured at 405 nm using the Thermo Scientific Genesys 10s Vis spectrophotometer.

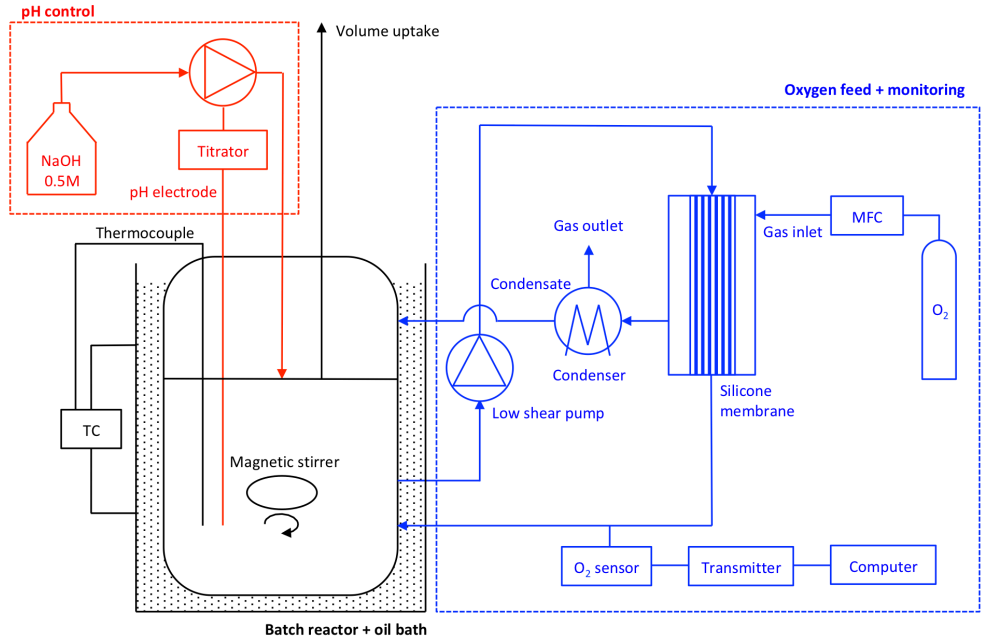

Figure S5. Process flow diagram of the experimental set-up used for the chemo-enzymatic epoxidation of allyl alcohol. In blue is enlighten the recirculation loop used to feed the reaction medium with oxygen and monitor the oxygen concentration, whereas the titration unit is represented in red. TC = temperature controller, MFC = mass flow controller.

1.5. Immobilization of horseradish peroxidase (HRP) and HRP/GOx mixture

Horseradish peroxidase (HRP), in powder form, was purchased from Sigma-Aldrich. This enzyme was immobilized on **TS-1_Aer** with a loading of 50 $mg.g^{-1}$ following the same procedure as **GOx** (see Section 1.3), starting from a 25 $mg.ml^{-1}$ HRP solution ("**HRP_25@TS-1_Aer**", see Figure S6a–b). Alternatively, HRP and **GOx** were co-immobilized on **TS-1_Aer** (combi-CLEAs). In this case, the **TS-1_Aer** solid was impregnated with a 25 $mg.mL^{-1}$ enzymatic solution containing 75 wt. % HRP and 25 wt. % **GOx** ("**HRP/GOx_25@TS-1_Aer**", see Figure S6e–f).

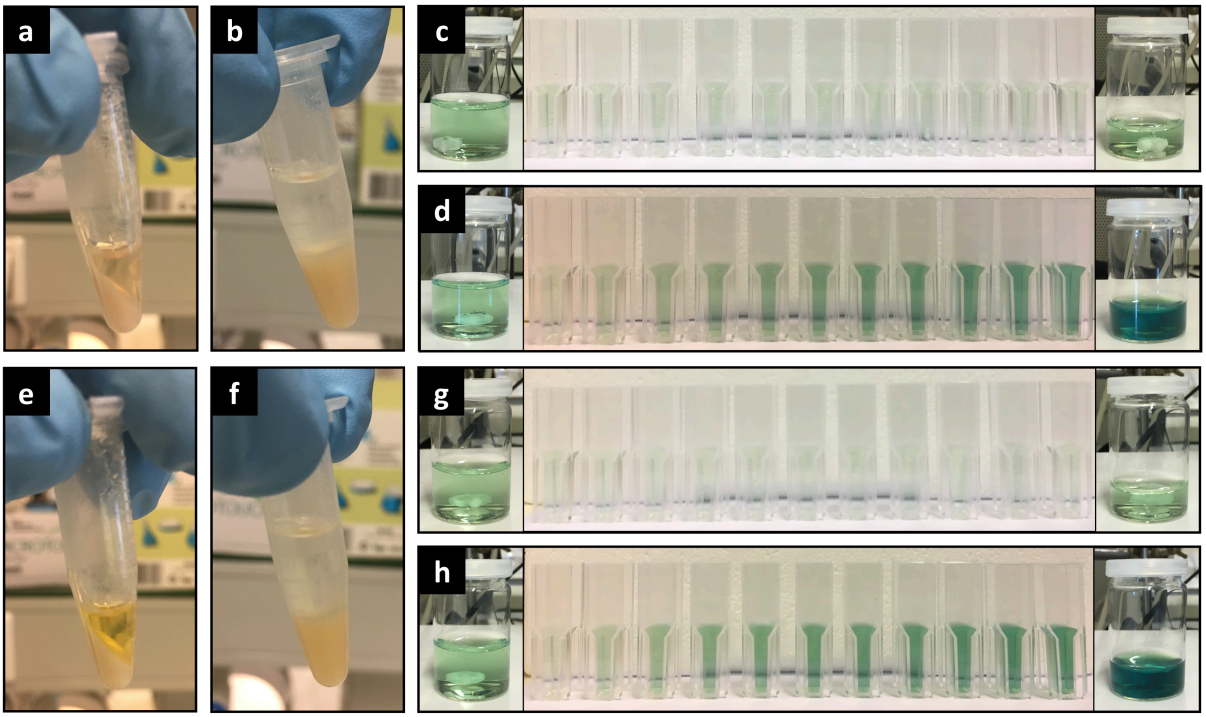

Figure S6. Preparation and testing of the **HRP_25@TS-1_Aer** (a–d) and **HRP/GOx_25@TS-1_Aer** (e–h) samples. Pictures illustrating the immobilization of the enzyme(s) are shown in (a–b) and (e–f) (see also Figure S3). In (a) and (e), the solid is respectively suspended in solutions of HRP and HRP/**GOx** (75:25 w/w) (impregnation step). In (b) and (f), the impregnated solids are recovered by centrifugation and suspended in a ethyl lactate/glutaraldehyde mixture (precipitation and cross-linking step). The colour of the pellet indicates the presence of enzymes in the solid: the brown colour is due to HRP whereas the yellow colour is due to **GOx**. In both cases, the supernatant is almost colorless. Colorimetric assays carried out on **HRP_25@TS-1_Aer** and **HRP/GOx_25@TS-1_Aer** are illustrated in (c–d) and (g–h), respectively. The coloration of the solution as a function of the production of $ABTS^{+\bullet}$ catalyzed by HRP is clearly visible in (d) and (h), whereas assays carried out on filtrated suspensions (c) and (g) (*i.e.* in the absence of solid) show no enzymatic activity.

The activity of HRP was assessed at room temperature (*ca*. 23°C) by a colorimetric assay in the presence of 2,2'-azino-bis(3-ethylbenzothiazoline-6-sulfonic acid) (ABTS) as substrate. For **HRP_25@TS-1_Aer** (Figure S6d), the reaction was initiated by adding 33 µl of suspension to 10 ml of citric acid-phosphate buffer (10 mM, pH 6.0) containing H_2O_2 (44 µM) and ABTS (3.2 mM). For **HRP/GOx_25@TS-1_Aer** (Figure S6h), H_2O_2 was replaced by D-glucose (200 mM) and the reaction medium was saturated with air for 1 min prior to the addition of the suspension. During the reaction, 500 µl aliquots were collected at regular time intervals and added to 33 µl of HCl 4 M, the latter being used to stop the reaction. Then, 500 µl of distilled water was added and the absorbance was measured at 405 nm (ε_{405} = 36,800 $M^{-1}cm^{-1}$). The concentration of $ABTS^{+\bullet}$ at each time was obtained using the Beer-Lambert law:

$$[ABTS^{+\bullet}]\ [M] = \frac{(A_{405}(t) - A_{405}(0))\ \frac{1.033\ [ml]}{0.500\ [ml]}}{36{,}800\ [M^{-1}cm^{-1}]\ 1\ [cm]}$$

In both experiments, the measured enzymatic activity of HRP was in the 9.0–9.4 $mU.ml^{-1}$ range (1 U corresponds to the oxidation of 1 µmol of ABTS per minute).

The enzyme heterogeneization was addressed by filtration tests (Figure S6c,g) carried out by removing the solid particles in the suspensions using a 0.2 µm syringe filter and then measuring the enzymatic activity in the filtrate as described above.

2. Results and Discussion

2.1. Additional figures

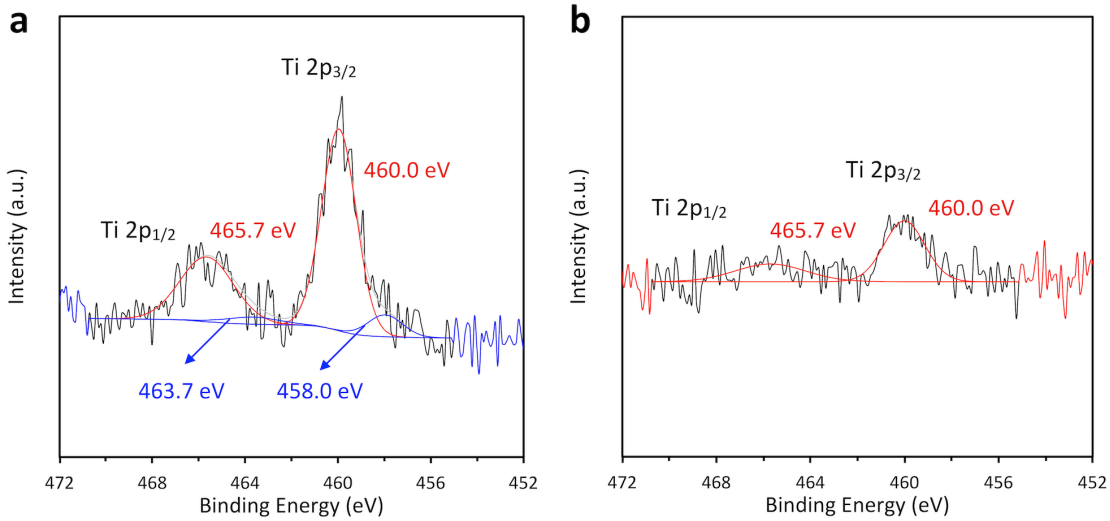

Figure S7. Decomposition of the XPS Ti 2p spectrum of (a) **TS-1** and (b) **TS-1_Aer**.

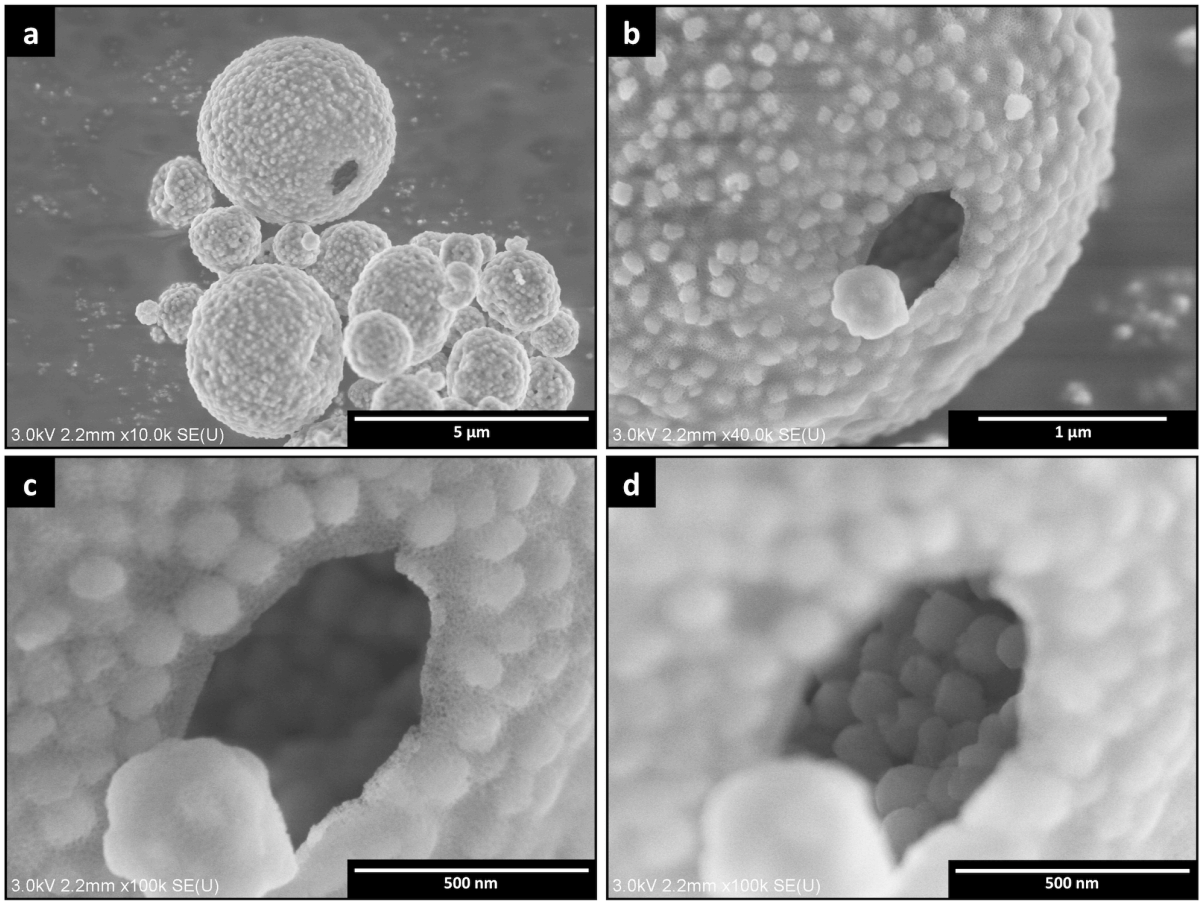

Figure S8. Additional SEM-FEG images of **TS-1_Aer** illustrating the shell morphology of the particles. Images in (a–c) were recorded at ×10k, ×40k and ×100k magnification, respectively. Images in (c–d) were taken at same magnification but on diferent focal planes, revealing respectively the outside and inside part of the shell.

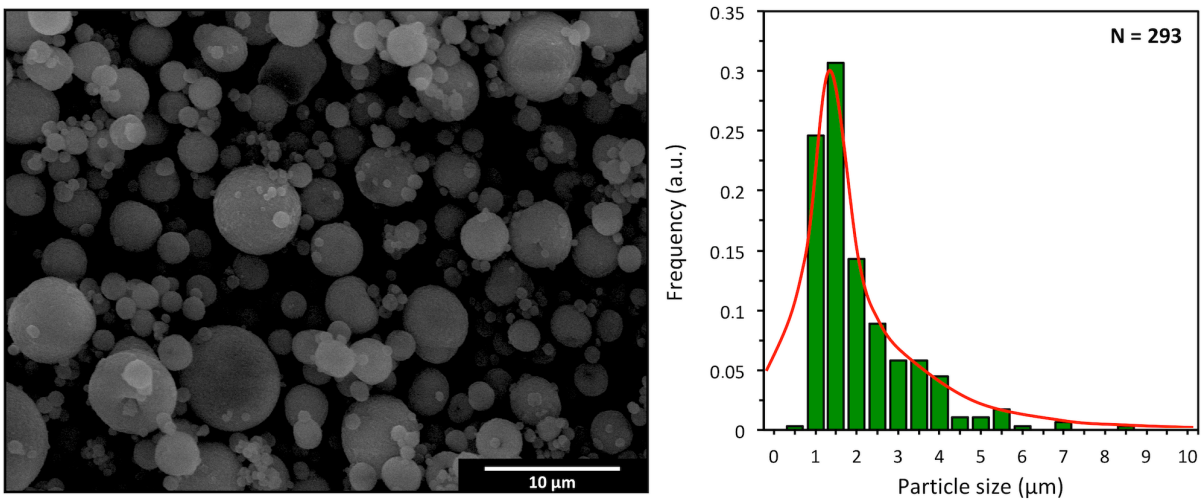

Figure S9. Particle size distribution of **TS-1_Aer** as determined from SEM imaging (recorded at low magnification).

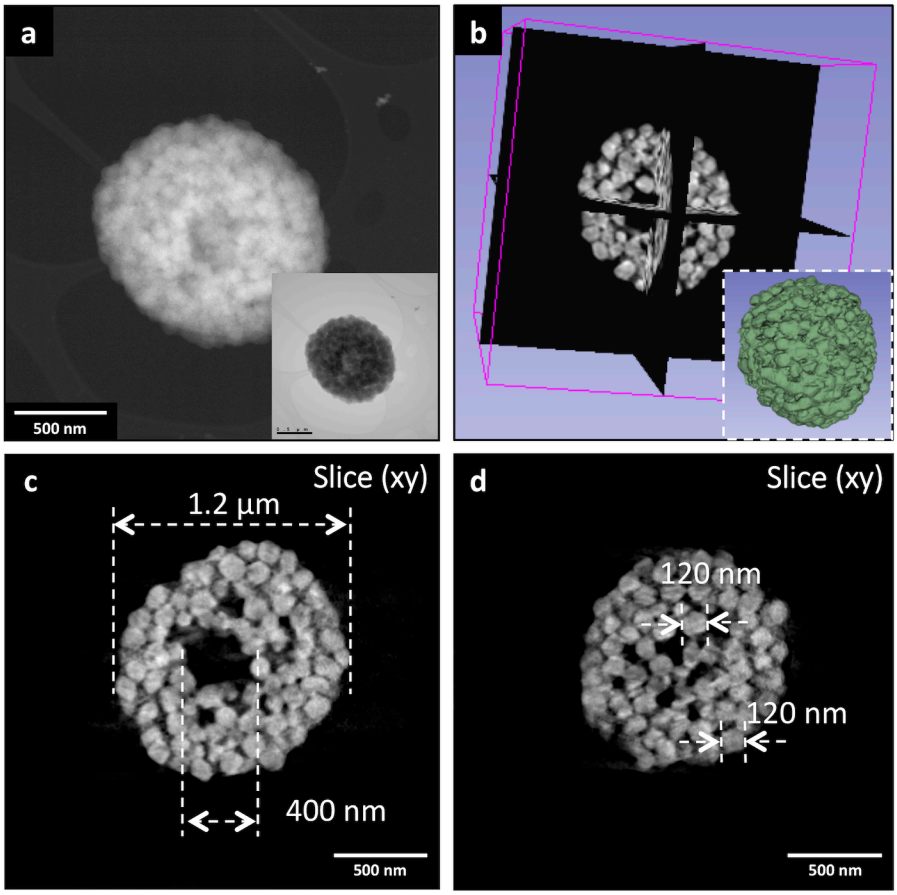

Figure S10. (a) STEM-ADF image (corresponding STEM-BF image in inset) of a typical **TS-1_Aer** particle of *ca.* 1.2 µm, (b) calculated 3D volume (3D model in inset), (c–d) representative (xy) slices extracted from the 3D volume.

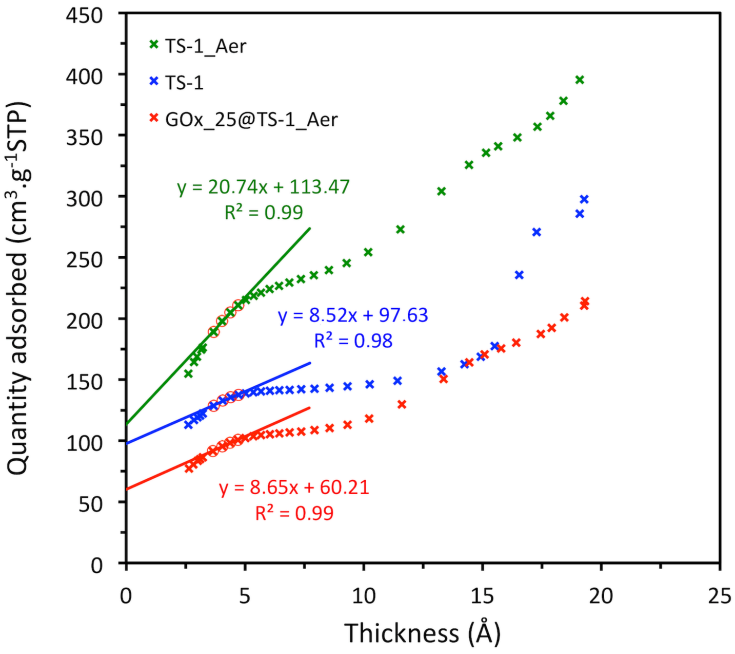

Figure S11. T-plots based on the adsorption branch of the isotherm of the catalysts. The external specific surface area – which includes the specific surface area of mesopores – is evaluated by the slope of the linear regression calculated in the 3.5–5 Å thickness range; the micropore volume is given by the intercept (density conversion factor = 0.0015468).

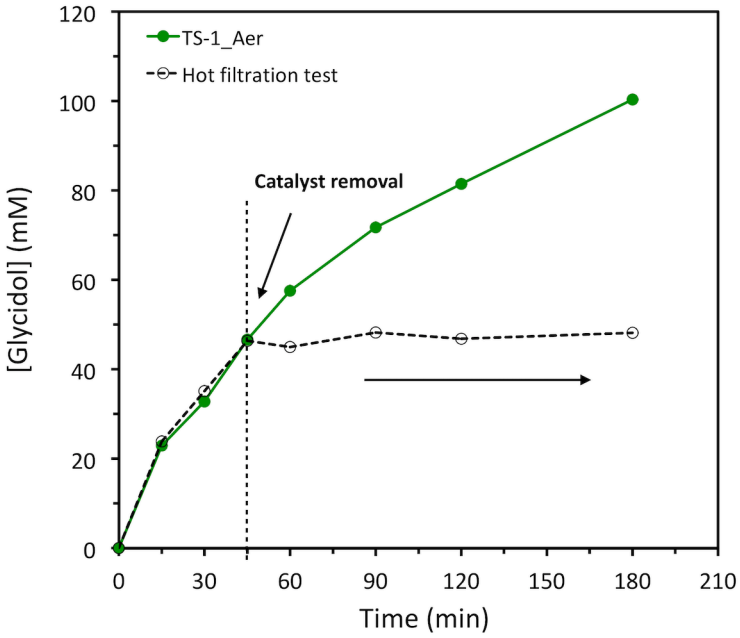

Figure S12. Hot filtration test for the epoxidation of allyl alcohol with H_2O_2 catalyzed by **TS-1_Aer**. No production after the removal of the solid catalyst at 45 min was observed. Experimental conditions: T = 45°C, [CATA] = 5 $g.l^{-1}$, [Allyl alcohol] = 0.9 M, [H_2O_2] = 0.18 M.

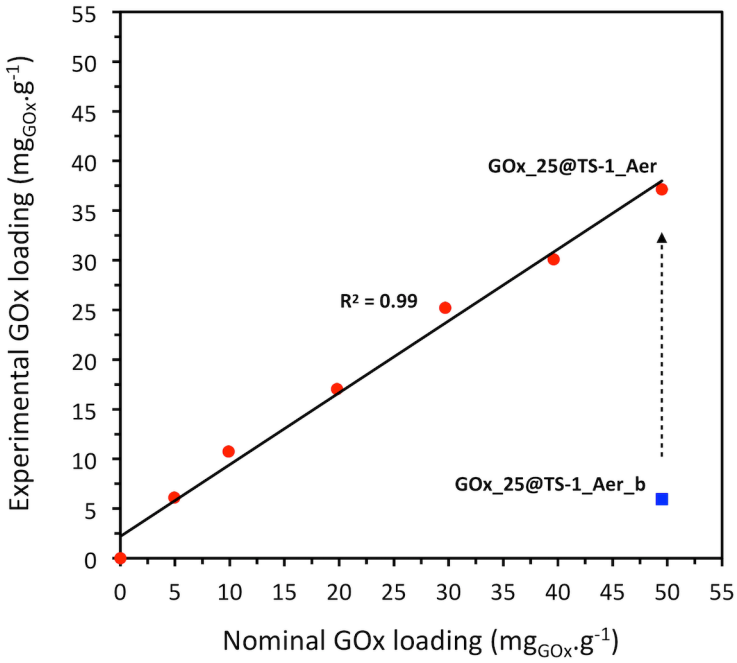

Figure S13. Experimental *vs.* nominal enzyme loadings in **GOx_X@TS-1_Aer.** The experimental loading of **GOx** in **GOx_25@TS-1_Aer_b** – prepared without precipitation and cross-linking agents – is shown for comparison.

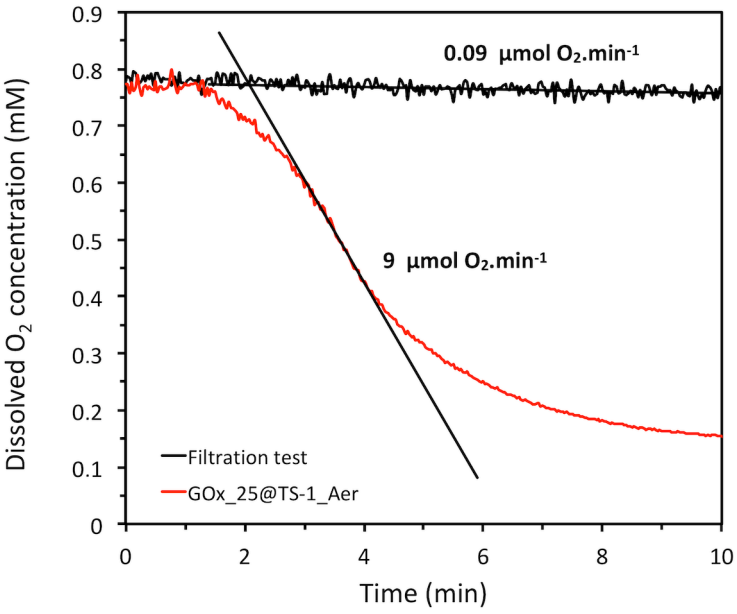

Figure S14. Filtration test for the **GOx** catalyzed consumption of oxygen using **GOx_25@TS-1_Aer**. The activity in the suspension (5mg of solid catalyst in 100 ml) is compared to the activity in the supernatant – obtained after centrifugation and filtration (0.2 µm). Experimental conditions: T = 45°C, 10 mM citric acid-phosphate buffer pH 6.0, [D-glucose] = 200 mM.

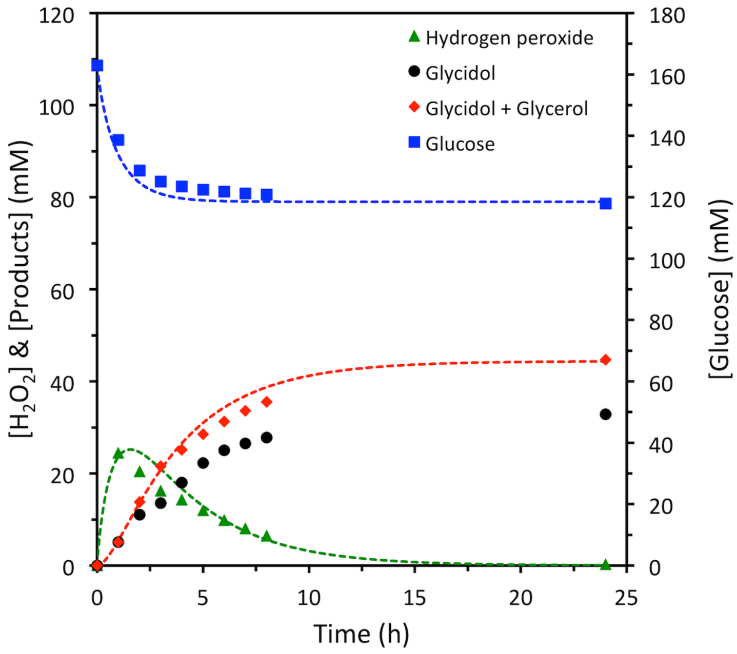

Figure S15. Reproducibility of the chemo-enzymatic cascade reaction evaluated on **GOx_25@TS-1_Aer**. The experimental conditions and parameters used in the mathematical model are identical to Figure 5b and Table S1 (see below), respectively.

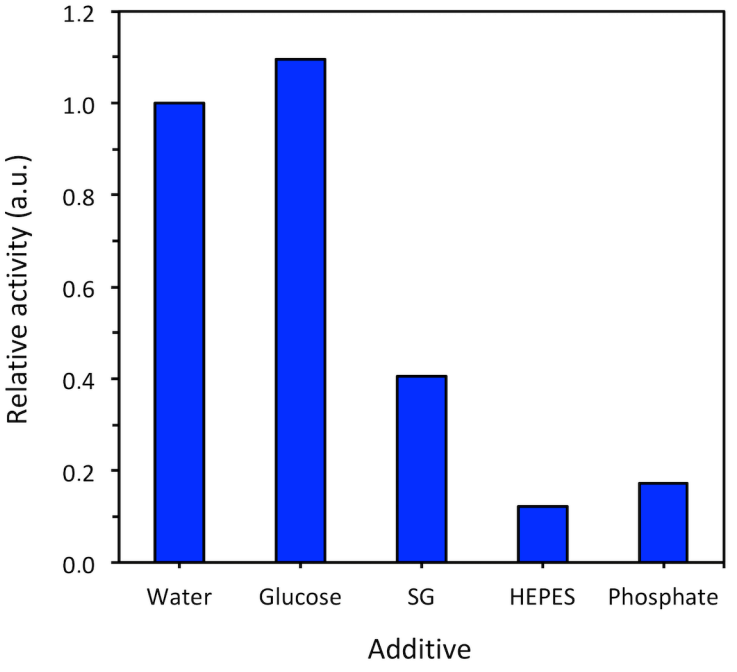

Figure S16. Effect of the presence of additives on the activity of **TS-1**. Data were collected in the initial stage of the reaction (45 min reaction time) and the catalytic activity (expressed in terms of glycidol production per g of catalyst) relative to the test carried out in water was calculated for each additive. Experimental conditions: : T = 45°C, [CATA] = 5 $g.l^{-1}$, [Allyl alcohol] = 0.9 M, [H_2O_2] = 0.18 M. The additive concentrations used were 100 mM for sodium gluconate (SG, pH 7.3) and buffers (HEPES and phosphate, resp. pH 7.0 and 7.3) and 200 mM for D-glucose. All additives – except glucose – were shown to have a detrimental impact on the catalytic activity of **TS-1**, as a result of the oxophilic nature of Ti(IV) species[15] which tend to strongly adsorb oxygen rich molecules possessing for example carboxylic, sulfonic or phosphoric groups. The competition of these molecules with H_2O_2 for the active site contributes to lower the activity of the epoxidation catalyst. Nevertheless, the relative activity in the presence of sodium gluconate was about three times higher than in HEPES and phosphate buffers, suggesting that gluconic acid titration is the most appropriate method to control acidification by the gluconic acid product during the cascade reaction.

2.2. Detailed description of the mathematical model used to approximate the chemo-enzymatic production of glycidol

A simplified mathematical model was created in Matlab (The MathWorks, USA) to describe the epoxide production through the cascade reaction in the presence of the hybrid catalysts.

$$Ti + H_2O \rightleftharpoons Ti{\bullet}H_2O \quad (S1)$$

$$Ti{\bullet}H_2O + H_2O_2 \overset{K_1}{\rightleftharpoons} Ti{\bullet}H_2O{\bullet}H_2O_2 \quad (S2)$$

$$Ti{\bullet}H_2O + \text{Allyl alcohol} \overset{K_2}{\rightleftharpoons} Ti{\bullet}H_2O{\bullet}\text{Allyl alcohol} \quad (S3)$$

$$Ti{\bullet}H_2O{\bullet}H_2O_2 + \text{Allyl alcohol} \overset{k}{\rightarrow} Ti{\bullet}H_2O{\bullet}\text{Glycidol} + H_2O \quad (S4)$$

$$Ti{\bullet}H_2O{\bullet}\text{Glycidol} \overset{K_3}{\rightleftharpoons} Ti{\bullet}H_2O + \text{Glycidol} \quad (S5)$$

A pseudo *Eley-Rideal* equation (Equation S6) – with olefin reacting with hydrogen peroxide adsorbed on the Ti active site – was used to establish the kinetic profile of the inorganic catalyst, as it is commonly reported for titanosilicate catalysts (Equation S1–S5).[16,17]

$$\frac{d[\text{Glycidol}]}{dt} = \frac{k_{app}K_1[H_2O_2][\text{Allyl alcohol}]}{1+K_1[H_2O_2]+K_2[\text{Allyl alcohol}]+K_3[\text{Glycidol}]} \quad [\text{Glycidol}]_0=0 \quad (S6)$$

with $k_{app} = k[CATA]$

k_{app} is defined as the reaction rate constant of the rate limiting step (Equation S4) – taking into account the catalyst concentration – whereas K_1, K_2 and K_3 are the equilibrium constants for reactions depicted in Equations S2, S3 and S5, respectively. Although the competition of the olefin with H_2O_2 for the active sites of **TS-1** has previously been reported to be low for propylene and allyl chloride epoxidation (*i.e.* $K_1 >> K_2$),[16,17] the high concentration of the olefin used (0.9 M) implies that the term K_2*[Allyl alcohol]* can be considered as a constant, with significant contribution to the kinetic model. The active sites were assumed to be coordinated with water molecules (Equation S1).[18]

A *Michaelis-Menten* equation applied to an enzymatic consumption of two substrates was previously reported to describe the kinetics of the enzymatic oxidation of β-D-glucose by **GOx** (Ping-Pong Bi-Bi mechanism). Taking into account the competitive inhibition by H_2O_2 proposed by Bao *et al.*,[8] the O_2 consumption rate by glucose oxidase was described *via* Equation S7.

$$\frac{d[O_2]}{dt} = -\frac{V_M[O_2]}{[O_2]+K_M\left(1+\frac{[H_2O_2]}{K_I}\right)} \quad [O_2]_0 = [O_2]_{sat} \quad (S7)$$

with $V_M = \frac{k_{CAT}[\text{Enzyme}]}{1+\frac{k_{mG}}{[\text{Glucose}]}}$ and $K_M = \frac{k_{mO}}{1+\frac{k_{mG}}{[\text{Glucose}]}} \approx K_I$

In Equation S7, V_M is the apparent maximum reaction rate, k_{CAT} is the rate constant of **GOx**, K_M is the apparent Michaelis constant with respect to oxygen and K_I the competitive inhibition constant by H_2O_2. k_{mG} and k_{mO} are the Michaelis constants with respect to D-glucose and oxygen, respectively. Since glucose was used in large excess (160–200 mM) as compared to value reported for k_{mG} (26 mM[6]), the latter parameter was considered as constant whatever the temperature and the form of the enzyme. From previously reported data, it was shown that H_2O_2 competition with O_2 for the enzyme active site implies that $K_M \approx K_I$.[8] As a consequence, Equation S7 was simplified as shown in Equation S8.

$$\frac{d[O_2]}{dt} = -\frac{V_M[O_2]}{[O_2]+K_M+[H_2O_2]} \quad [O_2]_0 = [O_2]_{sat} \quad (S8)$$

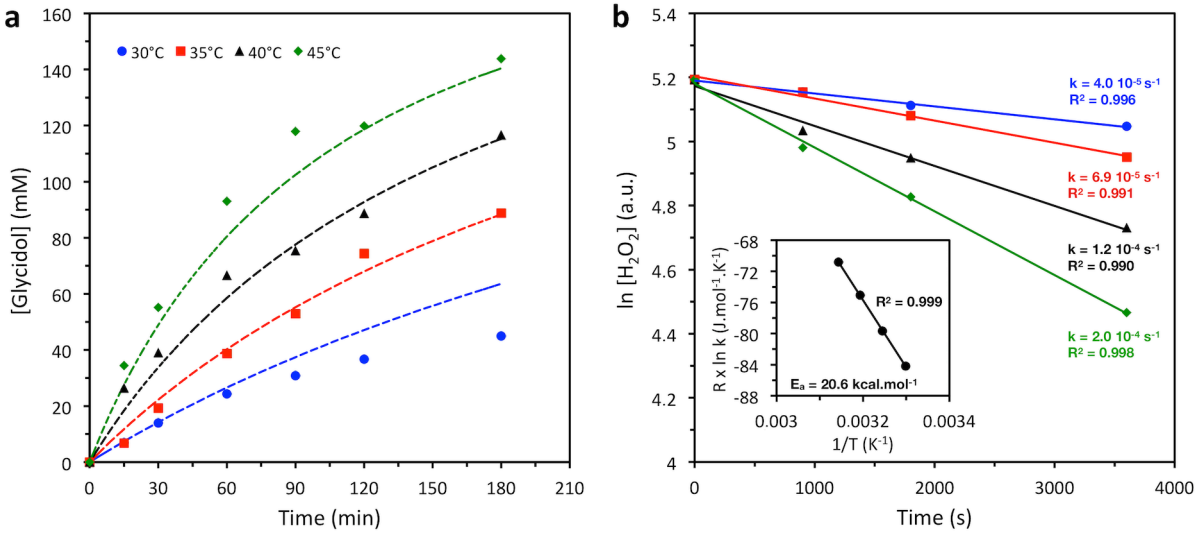

Figure S17. (a) Kinetic data for the **TS-1** catalyzed conversion of allyl alcohol into glycidol in H_2O using 30 wt. % aq. H_2O_2 as oxidant. Dashed lines represent the kinetic curves drawn from Equation S6 using the *k* constant determined by an initial rate analysis shown in (b) and *K* values from Liang *et al.*[17] Experimental conditions: [CATA] = 6.2 $g.l^{-1}$, [Allyl alcohol] = 0.9 M, [H_2O_2] = 0.18 M. As it is commonly accepted that enzymes preferentially work under mild conditions, the epoxidation activity was tested within 30–45°C temperature range in order to find a compromise for both catalytic partners. The results indicate that the reaction rate is the highest at 45°C within the temperature range tested. Since the enzyme was shown to withstand 45°C (see Figure 4d), the latter temperature was used to test the cascade reaction, (b) initial rate analysis;[19] the concentration of hydrogen peroxide at each time "[H_2O_2]" is here approximated by deducting the cumulative production of glycidol in (a) from the introduced amount of H_2O_2. In inset is illustrated the determination of the activation energy E_a – given by the slope of the Arrhenius plot. The obtained value of 20.6 kcal/mol is higher than the value of 9.3 kcal/mol reported by Hammond and Tarantino for the epoxidation of allyl alcohol by **TS-1** in methanol.[19] The higher energy barrier in the system **TS-1**/H_2O/H_2O_2 is tentatively ascribed to a rate inhibition of water. Indeed, Clerici *et al.* obtained much higher H_2O_2 conversion in methanol at 45°C, while using the same reactant concentrations.[20]

First, the value of *k* in the *Eley-Rideal* equation, as well as the values of k_{CAT} and K_M in the *Michaelis-Menten* equation, were evaluated by parameterization of Equation S6–S8 exploiting experimental data collected at various temperatures for **TS-1** (Figure S17) and free **GOx** (Figure S18a), respectively. The values of K_1, K_2 and K_3 were approximated using literature data for propylene epoxidation with H_2O_2 on **TS-1** (see Figure S17a).[17] Among these parameters, K_2 and K_3 are dependent on the nature of the olefin and the epoxide product. Their exact values for the epoxidation of allyl alcohol should ideally have been determined experimentally. Nevertheless, a parameter sensitivity analysis showed that K_2 and K_3 have little influence on the final solution of the model, confirming that the above approximation is valid.

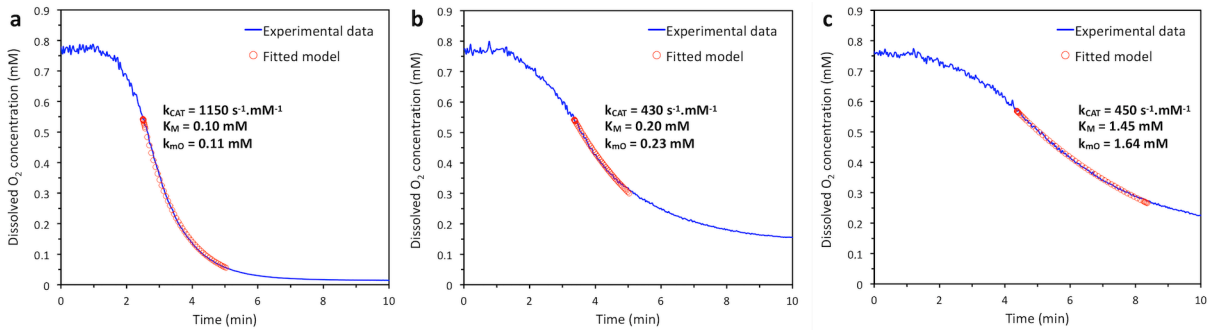

Figure S18. Fitting of the experimental data collected for the oxygen consumption by (a) free **GOx** (0.15 mg_{GOx}), (b) **GOx** in **GOX_25@TS-1_Aer** (0.19 mg_{GOx}) and (c) **GOx** in **GOx_2.5@TS-1_Aer** (0.26 mg_{GOx}). Experimental conditions: T = 45°C, 10 mM citric acid-phosphate buffer pH 6.0, [D-glucose] = 200 mM, 100 ml reaction medium. The enzyme is introduced at *ca.* 1 min.

Second, these values were used to parameterize Equation S6 when using **TS-1_Aer** and **GOx_25@TS-1_Aer** as catalysts in the epoxidation of allyl alcohol at 45°C, assuming that only the rate constant *k* is affected by the presence of the silica phase around individual **TS-1** crystals, whereas K_1, K_2 and K_3 are dependent on the surface chemistry of **TS-1** and were therefore assumed to be unchanged. The *k* value for **GOx_2.5@TS-1_Aer** was assumed to be equal to that of **GOx_25@TS-1_Aer**. Similarly, Equation S8 was parameterized with the hybrid catalysts (Figure S18b–c), with the hypothesis that not only V_M but also K_M could be affected by the enzyme immobilization, as the rigidification of the enzyme due to cross-linking may change the accessibility to individual active sites. Indeed, results from the fitting procedure in Figure S18 showed that the K_M value was 0.10 and 0.20 mM for the free and cross-linked enzyme in **GOx_25@TS-1_Aer**, respectively. This trend was previously reported for a cross-linked laccase.[21] In **GOx_2.5@TS-1_Aer**, K_M reached a very high value of 1.45 mM, whereas the k_{CAT} value barely changed. This is in accordance with

the hypothesis that at low enzyme loadings, the enzyme conformation is more constrained, thus explaining the low specific activity of the enzyme in **GOx_2.5@TS-1_Aer** (see Figure 4b).

Due to the high porosity of the solid shell, we assumed that there was no influence of diffusion on the epoxidation activity and enzyme kinetics. Similarly, diffusional limitations within each CLEA particle was neglected, although the occurrence of diffusional limitation should not be totally excluded since a higher K_M value was calculated for the cross-linked enzymes.

To address the epoxide production by the hybrid catalysts *via* the *in situ* H_2O_2 production by the enzyme and its consecutive consumption on the inorganic catalyst, Equation S6–S8 were combined in a single system of equations (Equation S9–S11). The decomposition of hydrogen peroxide was assumed to be negligible.

$$\frac{d[O_2]}{dt} = - \frac{V_M[O_2]}{[O_2]+K_M+[H_2O_2]} \qquad [O_2]_0 = [O_2]_{sat} \quad (S9)$$

$$\frac{d[H_2O_2]}{dt} = \frac{V_M[O_2]}{[O_2]+K_M+[H_2O_2]} - \frac{k_{app}\, K_1[H_2O_2]\,[\text{Allyl alcohol}]}{1+K_1[H_2O_2]+K_2[\text{Allyl alcohol}]+K_3[\text{Glycidol}]} \qquad [H_2O_2]_0 = 0 \quad (S10)$$

$$\frac{d[\text{Glycidol}]}{dt} = \frac{k_{app}\, K_1[H_2O_2]\,[\text{Allyl alcohol}]}{1+K_1[H_2O_2]+K_2[\text{Allyl alcohol}]+K_3[\text{Glycidol}]} \qquad [\text{Glycidol}]_0 = 0 \quad (S11)$$

In order to improve the model accuracy, two additional terms were added to the equation system above: i) an *aeration* term (Equation S12), taking into account the re-oxygenation of the reaction medium through membrane exchange, ii) a *temperature deactivation* term (Equation S13), reflecting the stability of glucose oxidase against time at 45°C.

$$\frac{d[O_2]}{dt} = k_L a\,([O_2]^* - [O_2]) \quad (S12)$$

$$E = \frac{d[O_2]}{dt} = \left[\frac{d[O_2]}{dt}\right]_0 e^{-k_d t} = E_0\, e^{-k_d t} \quad (S13)$$

Equation S12–S13 are both time-dependent and characterized by a mass transfer coefficient, k_La, and an enzyme deactivation constant, k_d, respectively.

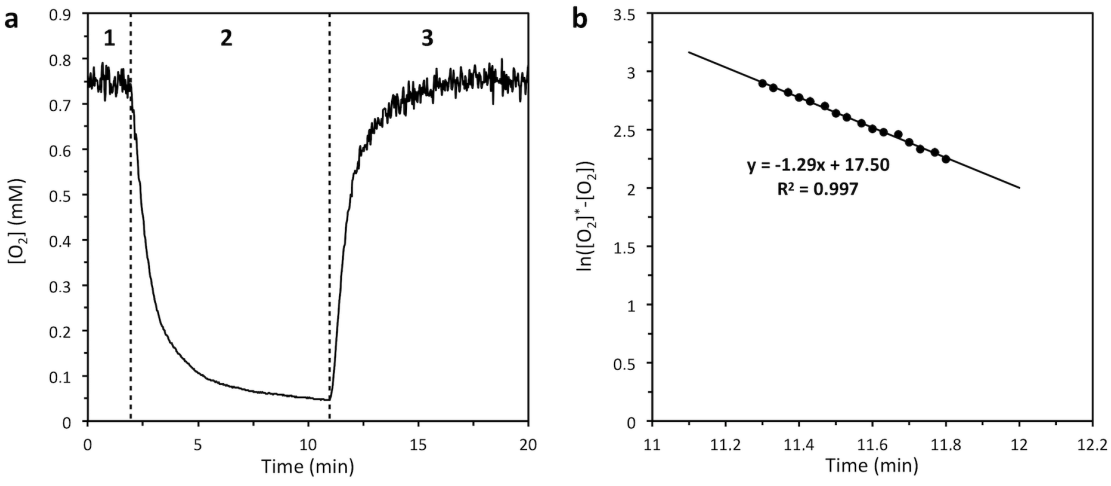

Figure S19. (a) Measurement of the mass transfer coefficient k_La *via* the optical oxygen sensor. The reaction medium was successively fed with oxygen (1), nitrogen (2) and oxygen (3) using the PDMS hollow fiber module (PDMSXA-2500, MedArray, USA). Conditions: 100 ml.min^{-1} liquid flow rate (lumen side), 1 l.h^{-1} sweep rate (shell side), (b) the mass transfer coefficient was evaluated at stage (3) using the linearized equation shown in Equation S14.

The mass transfer coefficient k_La (1.29 min^{-1}) was measured at 45°C with the optical oxygen sensor. The experiment consisted first in degassing the reaction medium with N_2, then switching to O_2 and measuring the oxygen uptake to deduce the value of k_La from Equation S14 (Figure S19).

$$\ln\left([O_2]^* - [O_2]\right) = -k_L a\, t \quad (S14)$$

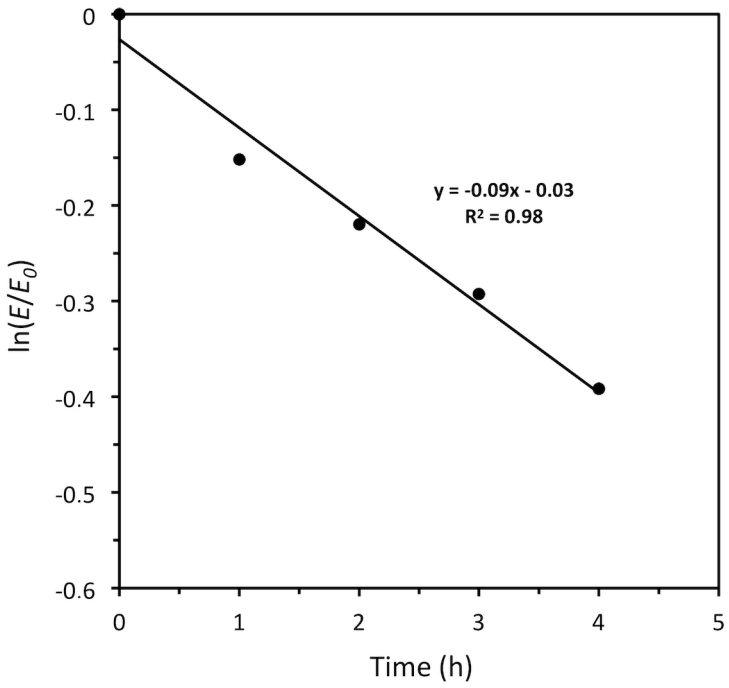

Figure S20. Determination of the deactivation constant k_d of free **GOx** by the linearized equation shown in Equation S15 (data from Figure 4d). The value of 0.09 h^{-1} corresponds to a half life of *ca.* 8h, which is lower than the value reported for laccase for example.[22]

The deactivation constant k_d at 45°C was calculated by reporting the enzymatic activity $E = \frac{d[O_2]}{dt}$ against time upon incubation at 45°C for the hybrid catalyst **GOx_25@TS-1_Aer** (k_d = 0 h^{-1}) and for the free enzyme (k_d = 0.09 h^{-1}, Figure S20) (Equation S15, see also Figure 4d).

$$\ln\left(\frac{E}{E_0}\right) = -k_d\, t \qquad \text{(S15)}$$

Combining Equation S12–S13 with Equation S9–S11, the reaction kinetics of the cascade reaction was deduced from the following system of equations:

$$\frac{d[O_2]}{dt} = -\frac{V_M[O_2]}{[O_2]+K_M+[H_2O_2]}e^{-k_d t} + k_L a\,([O_2]^*-[O_2]) \qquad [O_2]_0 = [O_2]_{sat} \quad \text{(S16)}$$

$$\frac{d[H_2O_2]}{dt} = \frac{V_M[O_2]}{[O_2]+K_M+[H_2O_2]}e^{-k_d t} - \frac{k_{app}\,K_1[H_2O_2]\,[\text{Allyl alcohol}]}{1+K_1[H_2O_2]+K_2[\text{Allyl alcohol}]+K_3[\text{Glycidol}]} \qquad [H_2O_2]_0 = 0 \quad \text{(S17)}$$

$$\frac{d[\text{Glycidol}]}{dt} = \frac{k_{app}\,K_1[H_2O_2]\,[\text{Allyl alcohol}]}{1+K_1[H_2O_2]+K_2[\text{Allyl alcohol}]+K_3[\text{Glycidol}]} \qquad [\text{Glycidol}]_0 = 0 \quad \text{(S18)}$$

Equation S18 does not take into account possible selectivity issues (*i.e.* production of glycerol) and therefore should be considered as the combined production rates of glycidol and glycerol. Finally, the glucose consumption by the enzyme can be approximated using Equation S19 along with Equation S16–S18.

$$\frac{d[\text{Glucose}]}{dt} = -\frac{V_M[O_2]}{[O_2]+K_M+[H_2O_2]}e^{-k_d t} \qquad [\text{Glucose}]_0 = [\text{Glucose}]_{initial} \quad \text{(S19)}$$

Table S1. Summary of the parameters used in the mathematical modeling of the chemo-enzymatic production of glycidol at 45°C.

	System		
	Free GOx + TS-1_Aer	**GOx_25@TS-1_Aer**[a]	**GOx_2.5@TS-1_Aer**
k_La (min^{-1})		1.29	
k_{mG} (mM)[b]		26	
k_{mO} (mM)	0.11	0.23	1.64
k_{cat} ($s^{-1}.mM_{GOX}^{-1}$)[c]	1150	430	450
k_d (h^{-1})[d]	0.09 (1.1)	0[e] (1.1)	n.m. (0.65)
K_1 (mM^{-1})[f]		0.00189	
K_2 (mM^{-1})[f]		0.00045	
K_3 (mM^{-1})[f]		0.00729	
k ($s^{-1}.(g_{CATA}.l^{-1})^{-1}$)	2.0×10^{-5}	1.6×10^{-5}	1.6×10^{-5}

[a] The same parameters were used in the repeated experiment carried out on **GOx_25@TS-1_Aer**. [b] From literature data.[6] [c] Determined at pH 6.0. [d] In brackets are given the values recalculated from experimental results (Figure 5). [e] For the immobilized enzyme in **GOx_25@TS-1_Aer**, the plot of $ln(E/E_0)$ *vs.* time gives an inconsistent positive deactivation constant, as the activity is roughly constant (see Figure 4d). [f] Hypothesis: theses values have been approximated by results of Liang *et al.* on the epoxidation of propylene over **TS-1** in isopropanol.[17]

References

1 A. Thangaraj, M. J. Eapen, S. Sivasanker and P. Ratnasamy, *Zeolites*, 1992, **12**, 943–950.
2 M. Jacquemin, M. J. Genet, E. M. Gaigneaux and D. P. Debecker, *ChemPhysChem*, 2013, **14**, 3618–3626.
3 B. M. Reddy, B. Chowdhury and P. G. Smirniotis, *Appl. Catal. Gen.*, 2001, **211**, 19–30.
4 B. Erdem, R. A. Hunsicker, G. W. Simmons, E. D. Sudol, V. L. Dimonie and M. S. El-Aasser, Langmuir, 2001, **17**, 2664–2669.
5 P. Demarche, C. Junghanns, I. Ardao and S. N. Agathos, *Eng. Life Sci.*, 2015, **15**, 804–814.
6 S. Hayashi and S. Nakamura, *Biochim. Biophys. Acta*, 1976, **438**, 37–48.
7 S. B. Bankar, M. V. Bule, R. S. Singhal and L. Ananthanarayan, *Biotechnol. Adv.*, 2009, **27**, 489–501.
8 J. Bao, K. Furumoto, M. Yoshimoto, K. Fukunaga and K. Nakao, *Biochem. Eng. J.*, 2003, **13**, 69–72.
9 S. Nakamura, S. Hayashi and K. Koga, *Biochim. Biophys. Acta*, 1976, **445**, 294–308.
10 R. Wilson and A. P. F. Turner, *Biosens. Bioelectron.*, 1992, **7**, 165–185.
11 M. M. Bradford, *Anal. Biochem.*, 1976, **72**, 248–254.
12 T. Zor and Z. Selinger, *Anal. Biochem.*, 1996, **236**, 302–308.
13 R. Schoevaart, M. W. Wolbers, M. Golubovic, M. Ottens, A. P. G. Kieboom, F. van Rantwijk, L. a. M. van der Wielen and R. A. Sheldon, *Biotechnol. Bioeng.*, 2004, **87**, 754–762.
14 J. H. Bowes and C. W. Cater, *J. R. Microsc. Soc.*, 1966, **85**, 193–200.
15 G. Eisenberg, *Ind. Eng. Chem. Anal. Ed.*, 1943, **15**, 327–328.
16 H. Gao, G. Lu, J. Suo and S. Li, *Appl. Catal. Gen.*, 1996, **138**, 27–38.
17 X. Liang, Z. Mi, Y. Wu, L. Wang and E. Xing, *React. Kinet. Catal. Lett.*, 2003, **80**, 207–215.
18 M. G. Clerici, *Kinet. Catal.,* 2015, **56**, 450–455.
19 C. Hammond and G. Tarantino, *Catalysts*, 2015, **5**, 2309–2323.
20 M. G. Clerici and P. Ingallina, *J. Catal.,* 1993, **140**, 71–83.
21 S. K. S. Patel, S. H. Choi, Y. C. Kang and J.-K. Lee, *Nanoscale*, 2016, **8**, 6728–6738.
22 R. R. Nair, P. Demarche and S. N. Agathos, *New Biotechnol.*, 2013, **30**, 814–823.